

Real-time resolving assembly graph by ONT long reads data

Son Hoang Nguyen^{1,*}, Minh Duc Cao², and Lachlan Coin^{1,*}

¹Institute for Molecular Bioscience, the University of Queensland, St Lucia, Brisbane, QLD 4072 Australia; ²4catalyzer

* To whom correspondence should be addressed. E-mails: l.coin@imb.uq.edu.au, s.hoangnguyen@imb.uq.edu.au

This manuscript was compiled on **November 19, 2019 18:40**

5

Abstract: A real-time assembly pipeline for Oxford Nanopore Technology (ONT) data is important for either saving sequencing resources or reducing turnaround time for data analyses. The previous approach from **npScarf** provided a greedy fast-response, auto-correct streaming algorithm for such task but was relatively prone to mis-assemblies compared to other graph-based methods. Here we present **npGraph**, a real-time hybrid assembly software using the assembly graph instead of the separated pre-assembly contigs. It is able to produce more complete genome assembly by resolving the path finding problem on the assembly graph using long reads as the traversing guide. The applications on synthetic and real data set of isolate genomes show improved accuracy while still maintain the required computational cost at very low level. In addition, the built-in graphical user interface (GUI) can provide users a comprehensive look-and-feel of the whole assembly process. The tool and source code is available at <https://github.com/hsnguyen/assembly>.

Keywords: hybrid assembly, assembly graph, real-time analysis, nanopore sequencing

Introduction

Streaming assembly methods had been proven to be useful in saving time and resources compared to the conventional batch algorithms with examples included *e.g.* **Faucet** [1] and **npScarf** [2]. The first method allows the assembly graph to be constructed incrementally as long as reads are retrieved and processed. This practice is helpful dealing with huge short-read data set because it can significantly reduce the local storage for the reads, as well as save time for a De Bruijn graph (DBG) construction while waiting for the data being retrieved. **npScarf**, on the other hand, is a hybrid assembler working on a pre-assembly set of short-read assembly contigs. It functions by scaffolding the contigs using nanopore sequencing which is well-known by the real-time property. The completion of genome assembly in parallel with the sequencing run provides explicit benefits in term of resource control and turn-around time for analysis [2].

10

15

Hybrid approaches are still common practice in genome assembly and data analyses when Illumina sequencing remains the most favoured option in terms of cost and accuracy to date. On the other hand, the third-generation sequencing methods such as Pacbio or Oxford Nanopore Technology are well-known for the ability to produce much longer reads that can further complete the former's assembly. As the consequence, it is rational to combine two sources of data together in a hybrid method that can offer accurate and complete genomes at the same time. **npScarf**, following that philosophy, had been developed and deployed on real microbial genomes.

20

However, due to the greedy bridging approach of the contigs-based streaming algorithm, **npScarf**'s concurrent results might suffer from mis-assemblies [3, 4]. A default setting were optimized for microbial genomes input but cannot fit for all data from various experiments in practice. Also, the gap filling step has to rely on the low quality nanopore reads thus the accuracy of the final assembly is affected as well. To tackle the quality issue while maintaining its streaming execution, a bridging method by assembly graph traversing is proposed. In which, after the construction of a compact DBG assembly graph, the next step is to traverse the graph, resolve the repeats and identify the longest possible un-branched paths that would represents contigs for the final assembly.

25

30

Hybrid assembler using nanopore data to resolve the graph has been implemented in **hybridSPAdes** [5] or **Unicycler** [3]. In general, the available tools employ batch-mode algorithms on the whole long-read data set to generate the final genome assembly. In which, the **SPAdes** hybrid assembly module, from its first step, exhaustively looks for the most likely paths (with minimum edit distance) on the graph for each of the long read given but only ones supported by at least two reads are attained. In the next step, these paths will be subjected to a decision-rule algorithm, namely **exSPAndeR** [6], for repeat resolution by step-by-step expansion, before output the final assembly. On the other hand, **Unicycler**'s hybrid assembler will initially generate a consensus long read for each of the bridge from the batch data. The higher quality consensus reads are used to align with the assembly graph to find the best paths bridging pairs of anchored contigs. While the latter method employs the completeness of the data set from the very beginning for a consensus step, the former only iterates over the batch of possible paths and relies on a scoring system for the final decision of graph traversal. For that reason, the first direction is more suitable for a real-time pipeline.

35

40

Nonetheless, the challenges to adapt this approach into a real-time mechanism are obvious, mainly from building a progressive, self-updating path-finding and graph reducing method which are required for a streaming assembler on graph. A modified DFS (depth-first search) algorithm and a progressive voting algorithm has been implemented to overcome these issues. The method is implemented in **npGraph**, a user-friendly tool with GUI that can traverse the assembly graph and bridge its components in real-time as long as the nanopore sequencing process is still running.

45

Results

npGraph – a tool to resolve assembly graph in real-time

npGraph's input consists of Illumina assembly graph resulted from running assembler, e.g. SPAdes [7], Velvet [8], AbySS [9] on Illumina short reads, together with long reads from third generation sequencing technology (Oxford Nanopore Technology, Pacbio). The long reads will be aligned with the contigs in the assembly graph to indicate longer paths that should be traversed. These local paths, given sufficient data, are expected to untangle the complicated graph and guide to the global Eulerian paths (or cycles if possible) that represent the entire genomic sequences. npGraph can be invoked and fully function from the command-line interface. In addition, in order to aid the visualization of the assembly process, a GUI has been developed as well.

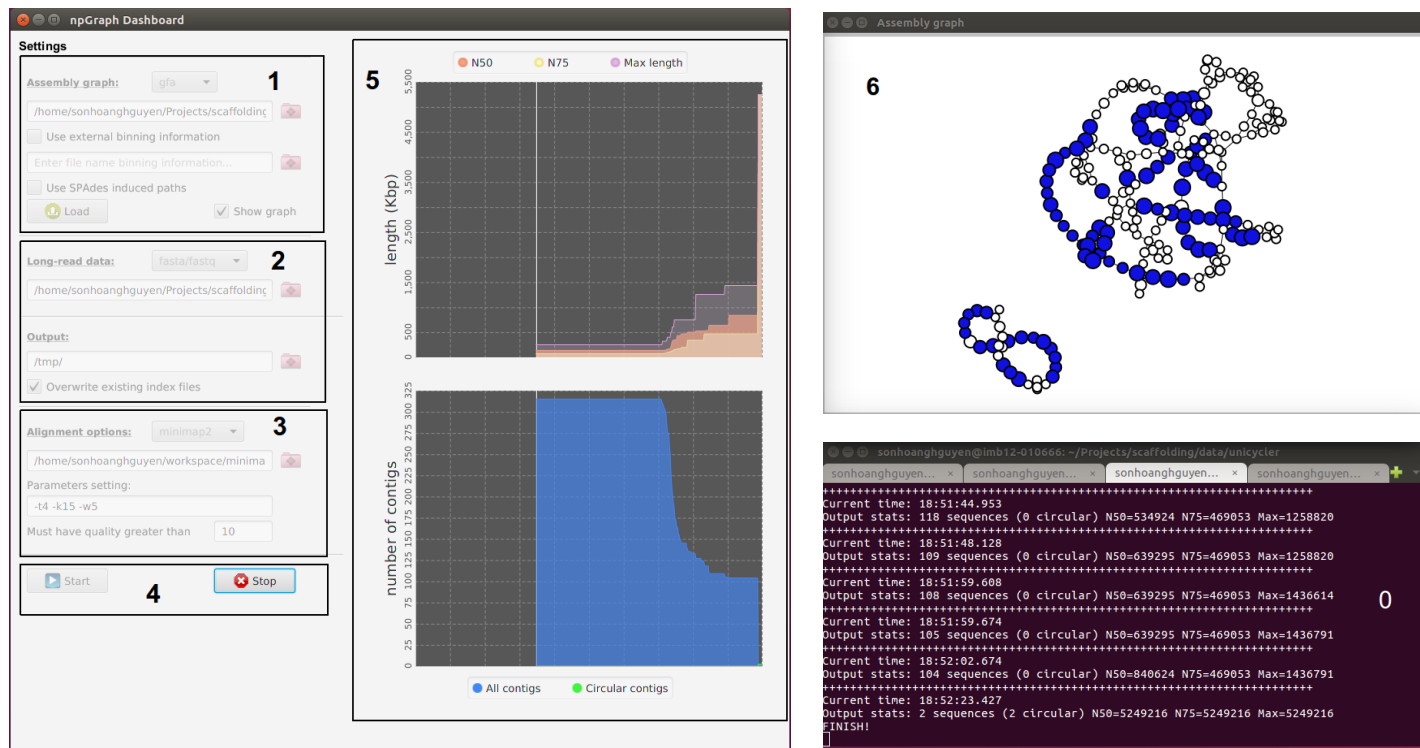


Figure 1: npGraph user interface including Console (0) and GUI components (1-6). The GUI consists of the Dashboard (1-5) and the Graph View (6). From the Dashboard there are 5 components as follow: 1 the assembly graph input field; 2 the long reads input field; 3 the aligner settings field; 4 control buttons (start/stop) to monitor the real-time scaffolding process; 5 the statistics plots for the assembly result.

The GUI includes the dashboard for control the settings of the program and another pop-up window for a simple visualization of the assembly graph in real-time (Figure 1). In this interface, the assembly graph loading stage is separated from the actual assembly process so that users can check for the graph quality first before carry out any further tasks. The box numbered 1 on Figure 1 is designed for this task. Only after an assembly graph is loaded successfully, users can move to box 2 to specify the nanopore input data. Settings for an aligner (BWA-MEM or minimap2) in box 3 is required if the input is the raw sequences in FASTA/FASTQ format. Another option is to run the alignment independently and provide SAM/BAM input for the next stage of bridging and assembly. This stage is controlled by buttons in box 4: the START button ignites the process while the STOP button can prematurely terminate it and output the assembly result till that moment. The plots from the right panel (5) depicts real-time statistics of the assembly contigs inferred from the graph. From the second window (6), the colored vertices imply unique contigs while the white ones involve either unspecified or repetitive elements. The number of different colors (other than white) indicates the amount of abundant groups being detected as population bins (e.g. chromosome versus different plasmids, or different bins in metagenomics).

A proper combination of command line and GUI can provide an useful streaming pipeline that copes well with MinION output data. The practice is similar to the previous developed pipelines [2, 10, 11] that allow the analysis to take place abreast to a nanopore sequencing run.

Evaluation using synthetic data

To evaluate the performance of the method, npGraph was tested against SPAdes with its hybrid assembly module [5], npScarf with/without assembly graph integrated, and Unicycler version 0.4.6 on Unicycler's synthetic data set [3]

. The data set is a simulation of Illumina and MinION raw data, generated *in silico* based on random and available microbial references. We ran all hybrid assembly methods in batch-mode and the reciprocal results were examined by QUAST 5.0.2 [14].

Table 1: Comparison of assemblies produced in batch-mode using npGraph and the comparative methods on 5 synthetic data sets taken from <https://cloudstor.aarnet.edu.au/plus/index.php/s/dzRCaxLjpGpfKYW>

Method	Assembly size (Mb)	#Contigs	N50 (Kp)	Mis-assemblies	Error (per 100 Kb)	Run times (CPU hrs)
random sequence with repeats						
SPAdes	3.928	226	40.5	0	0.00	0.95
SPAdes-Hybrid	4.109	3	4,000.0	0	0.85	1.196
Unicycler	4.110	3	4,000.0	0	0.47	6.783
npScarf	4.251	9	3,952.2	27	8.74	0.95 + 0.39
npScarf_wag	4.554	9	3,999.6	37	6.16	0.95 + 0.45
npGraph (bwa)	4.110	3	4,000.0	0	0.47	0.95 + 0.33
ngGraph (minimap2)	4.110	3	4,000.0	0	0.47	0.95 + 0.02
<i>Mycobacterium tuberculosis</i> H37Rv						
SPAdes	4.371	114	125.5	1	1.51	1.55
SPAdes-Hybrid	4.411	1	4,411.2	0	1.73	1.68
Unicycler	4.412	1	4,411.5	0	2.56	6.36
npScarf	4.446	4	4,389.9	12	11.41	1.55 + 0.78
npScarf_wag	4.408	1	4,407.6	2	7.01	1.55 + 0.79
npGraph (bwa)	4.411	1	4,411.6	0	7.28	1.55 + 0.63
ngGraph (minimap2)	4.411	1	4,411.4	0	7.01	1.55 + 0.02
<i>E. coli</i> O25b H4-ST131						
SPAdes	5.173	159	191.0	1	1.69	1.26
SPAdes-Hybrid	5.249	7	5,109.6	0	2.65	1.40
Unicycler	5.249	3	5,109.8	0	4.29	4.70
npScarf	5.354	7	5,087.5	14	29.12	1.26 + 0.78
npScarf_wag	5.413	7	5,108.1	6	30.29	1.26 + 0.78
npGraph (bwa)	5.252	3	5,112.3	0	16.37	1.26 + 0.66
ngGraph (minimap2)	5.250	3	5,111.1	0	14.61	1.26 + 0.03
<i>Streptococcus suis</i> BM407						
SPAdes	2.119	81	131.0	0	3.84	0.59
SPAdes-Hybrid	2.147	48	1,438.0	0	0.98	0.65
Unicycler	2.171	2	2,146.2	0	2.99	2.58
npScarf	2.220	4	2,120.0	9	97.20	0.59 + 0.31
npScarf_wag	2.245	4	2,128.3	3	89.64	0.59 + 0.31
npGraph (bwa)	2.167	6	2,146.7	0	26.77	0.59 + 0.21
ngGraph (minimap2)	2.167	6	2,146.2	0	22.53	0.59 + 0.01
<i>Acinetobacter</i> AB30						
SPAdes	4.134	265	42.5	0	3.23	0.95
SPAdes-Hybrid	4.287	49	3,308.0	0	5.04	1.84
Unicycler	4.333	1	4,333.0	1	6.95	5.27
npScarf	4.595	11	4,299.7	1	120.99	0.95 + 0.45
npScarf_wag	-	-	-	-	-	-
npGraph (bwa)	4.317	6	2,766.9	1	39.82	0.95 + 0.41
ngGraph (minimap2)	4.337	1	4,336.8	0	24.71	0.95 + 0.03

Table 1 shows comparative results running different methods on 5 synthetic data sets, the output of the full run can be found in Supplementary Table 1. In the first column of applied methods, beside Unicycler and hybridSPAdes, the original scaffolder npScarf was included as well as npScarf_wag – its modified version with assembly graph integrated. On the other hand, npGraph can use 2 different aligners, BWA-MEM and minimap2, for its bridging phase thus both practices were included in this comparison.

In general, the graph version of npScarf improved the assembly results in terms of mis-assemblies and error reduction while virtually consuming similar resources compared to the original version. The only exception where the number of mis-assemblies being increased was the simulation of a random sequence with many repeats. There were 10 more mistakes detected using the later version npScarf_wag. However, with additional investigations, we found that the number of mis-assemblies on the true positive circular sequences (3 from the reference) has been significant reduced by

applying assembly graph for **npScarf**. The errors mostly came from redundant sequences output from the software due to the failure in estimation of contig multiplicity. Even though using assembly graph for gap fillings, there were no changes in the way **npScarf_wag** determine if a contig is unique or not. Its implementation still relied on the length and coverage statistics, *i.e.* *Astats* [15] to find anchors that were critical for the backbone construction of the assembly. Redundant path findings for false positive replicons consequently returned additional wrong translocations in the final contigs which were reported by QUAST. Other than that, the method had successfully produced better assemblies than the original. Regarding *Mycobacterium tuberculosis* H37Rv, the number of mis-assembled breakpoints had been trimmed down from 12 to 2, while the number of final contigs had reduced from 4 to only one as in the reference. Results in cases of *E. coli* O25b H4ST131 and *Streptococcus suis* BM407 also showed enhancements in terms of those categories as well as N50 statistics. There was improvements considering the nucleotide errors (mismatches and indels) as well from aforementioned data sets, except for the *E. coli* when slightly more mismatches had been detected. However, these errors can be corrected by running polishing tools with the raw Illumina data afterward.

For *Acinetobacter* AB30 synthetic data, it was an deficiency for **npScarf_wag** in traversing the graph to find candidate paths for a bridge of long distance due to particular large search space. The exhaustive, naive DFS implementation for this version of **npScarf** required a lot of memory to traverse a complex assembly graph that usually exceed a normal desktop's capacity. This issue has been fixed in **npGraph** when Algorithm 1 was used on the definitive graph. This resulted in completed runs of the assembly process for all data sets with the similar number of mis-assemblies compared to the best figures in this category. As shown in Table 1 and 1, the assembly graph based methods offered significant improvements when compared to **npScarf**. Not only because of the clear drops with respect to mis-assemblies and errors, but it was also reflected by the number of final contigs and their N50 as well.

To align the long reads to the assembly graph components, either BWA-MEM [16] or minimap2 [17] was invoked in **npGraph**. The former option was inherited from **npScarf** pipeline with the intact parameters while the latter was used with the recommended settings (-k15 -w5) for the best sensitivity working on MinION data. Even though, BWA-MEM normally reported more hits than minimap2 but at the same time, was responsible for more false positive alignments. For instance, regarding the last data set from Table 1, the assembly of **npGraph** using BWA-MEM was suffered from the ambiguous alignments thus more fragmented than the other counterparts. On the other hand, referring to more complicated graphs from *Acinetobacter* A1 and the yeast *Saccharomyces cerevisiae* S288c from Table 1, the number of mis-assemblies from using minimap2 were increased due to the lacks of appropriate alignments to support accurate bridging process. However, under almost circumstances, using either aligners would result in final assemblies with similar qualities. Furthermore, in terms of running time and resources required, minimap2 proved to be the best option. The total CPU hours had been cut down drastically with the new aligner, making **npGraph** the fastest hybrid assembler available. This feature is certainly more favoured to a real-time assembly as well. As the consequence, as long as minimap2 is expected to replace BWA-MEM for long-read sequencing data alignment, it would likewise become the main aligner for **npGraph** pipeline in the future.

To evaluate assembly errors, we considered the measure of the total mismatches and indels per 100kbp from the assembly sequences when mapping to the reference. As expected from hybrid assembly method embedding Illumina data, the figures were hardly bigger than 100 (equivalent to 0.1% error rate) in almost every cases. Furthermore, the indels errors, which mainly caused by TGS data, were found relatively low in the final contigs (Table 1). The majority of the differences accounted for the mismatched nucleotides caused by the alternative paths connecting the unique anchors from the backbone of the assembly. This phenomenon may root from homologous repeats or sequencing errors of the genome. From all the hybrid assemblers, **hybridSPAdes** reported results with highest fidelity. This meant that the performance its decision-rule algorithm **exSPander** [6] was the most accurate amongst all path finding methods. As the trade-off, there were fewer connections satisfying its quality threshold, resulting in the fragmented assemblies in cases of *Streptococcus suis* or *Acinetobacter* samples (Table 1 and 1). **Unicycler**, which employs an algorithm based on semi-global (or glocal) alignments [18] with the consensus long reads, returned the second best reliable and at the same time, closest-to-complete results overall. **npScarf**, on the other hand, exploited the long reads for the gap filling thus inherited the high error rates from them. By integrating the assembly graph for the task, the errors were reduced in general (random sequences, *M. tuberculosis*, *S. suis* from Table 1) but not completely since the mis-placed contigs were still not resolved in other circumstances. **npGraph** significantly reduced the errors compared to **npScarf**, however the figures were still higher than the those of the best counterparts. This implied a more robust decision making system is needed in **npGraph**'s real-time path finding module for even better output's accuracy.

Hybrid assembly for real data sets

A number of sequencing data sets from *in vitro* bacterial samples [19] were used in this scenario. The data included both Illumina paired-end reads and MinION sequencing based-call data for each sample. Due to the unavailability of reference genomes, there were fewer statistics being reported by QUAST for the comparison of the results. Instead, we investigated the number of circular sequences and **PlasmidFinder** 1.3 [20] mappings to obtain an evaluation on the accuracy and completeness of the assemblies. Table 2 shows the benchmark results of **npGraph** (using minimap2) against **Unicycler** on three data sets of bacterial species *Citrobacter freundii*, *Enterobacter cloacae* and *Klebsiella oxytoca*.

From the first data set, there was high similarity between final contigs generated by two assemblers. They shared the same number of circular ultimate sequences, including the chromosomal and other six replicons contigs. The only

Table 2: Assembly of real data sets using **Unicycler** and **npGraph** with the optimized **SPAdes** output. Circular contigs are highlighted in **bold**, fragmented assemblies are presented as X|Y where X is the total length and Y is the number of supposed contigs making up X.

	Unicycler	npGraph	Replicons (based on PlasmidFinder 1.3)
<i>Citrobacter freundii</i> CAV1374	5,029,534 109688 100,873 85,575 43,621 3,223 1,916 14,464 3	5,029,486 109688 100,873 85,575 43,621 3,223 1,916 14,456 2	Chromosome IncFIB(pHCM2)_1_pHCM2_AL513384 IncFIB(pB171)_1_pB171_AB024946 IncL/M(pMU407)_1_pMU407_U27345 repA_1_pKPC-2_CP013325 - ColRNAI_1_DQ298019 -
<i>Enterobacter cloacae</i> CAV1411	4,806,666 2 90,451 33,610 13,129 2	4,858,438 2 90,693 2 33,610 14,542 4	Chromosome IncR_1_DQ449578 repA_1_pKPC-2_CP013325 -
<i>Klebsiella oxytoca</i> CAV1015	6,153,947 5 113,105 111,395 108,418 76,183 11,638	6,155,762 113,105 111,395 109,209 13 76,186 11,892 2	Chromosome IncFII(SARC14)_1_SARC14_JQ418540; IncFII(S)_1_CP000858 - IncFIB(K)_1_Kpn3_JN233704 IncL/M(pMU407)_1_pMU407_U27345 -

divergence lied on the biggest sequence ($\simeq 5.029\text{Mbp}$) when the **Unicycler**'s chromosome was 48 nucleotides longer than that of **npGraph**. Five out of six identical replicons were confirmed as plasmids based on the occurrences of appropriate Origin of replication sequences (PlasmidFinder database). In detail, two megaplasms (longer than 100Kbp) were classified as IncFIB while the other two mid-size replicons, 85.6Kbp and 43.6Kbp, were incL and repA respectively, leaving the shortest one with 2Kbp of length as ColRNAI plasmid. The remaining circular sequence without any hits to the database was 3.2Kbp long suggesting that it could be phage or newly replicon's DNA. Lastly, there were still 14.5Kbp unfinished sequences resulted in 3 linear contigs from **Unicycler** and 2 for **npGraph** respectively.

The assembly task for *Enterobacter cloacae* was observed more challenging as the chromosomal DNA sequence not been fully resolved using either method. The chromosome size was estimated to be approximately 4.8Mbp but had been broken into two smaller pieces. **npGraph** returned longer stretches of length 3.324Mbp and 1.534Mbp while the figures were 2.829Mbp and 1.978Mbp from **Unicycler**'s output. However, the number of circular sequences detected by **Unicycler** was one more than the other (2 versus 1). They were corresponding to 2 plasmids, namely IncR and repA. While the latter were recognized by both methods, the longer plasmid sequence was fragmented running **npGraph**. Similar to the previous data set, there were around 14Kbp of data were unable to be finished by the assemblers.

Finally, assembly for *Klebsiella oxytoca* saw fragmented chromosome using **Unicycler** but it was a fully complete contig for **npGraph** with 6.156Mbp of size. The two assemblers shared 3 common circular sequences where two of them were confirmed plasmids. The first identical sequences represented a megaplasms ($\simeq 113\text{Kbp}$) with two variations of IncFII's origin of replication DNA being identified. The other agreed plasmid were IncL/M with 76Kbp of length. Particularly, there was one circular contig with length greater than 100Kbp but returned no hits to the plasmid database, suggesting the importance of *de novo* replicon assembly in combination with further interrogations. **Unicycler** detected another megaplasms of size 108.4Kbp which was fractured by **npGraph**. The dissolution was also observed in **npGraph** for the final contig of length 11.6Kbp where it failed to combine two smaller sequences into one.

In addition to what presented in Table 2, dot plots for the pair-wise alignments between the assembly contigs were generated and can be found in Appendix Figure 1. Interestingly, beside all other agreements, there was a structural difference using two methods for *E. cloacae* CAV1411 genome assembly. This was caused by the inconsistency of a fragment's direction on the final output contigs. However, when compare to a reference genome of the same bacteria strain (GenBank ID: CP011581.1 [21]), contigs generated by **npGraph** demonstrated a consistent alignment which was not the case for **Unicycler** results (Appendix Figure 2). Even though this might reflect a novel variation between bacterial samples of the same strain, it was more likely a mis-assembly by using **Unicycler**.

Overall, by testing with synthetic and real data, **npGraph** proved to be able to generate assemblies of comparative quality compared to other powerful batch-mode hybrid assemblers, such as **hybridSPAdes** or **Unicycler**. Furthermore, similar to **npScarf**, it has the advantage in term of supporting real-time assembly. The next section will address this utility and the interactive GUI bundled in **npGraph**.

Assembly performance on streaming data

Figure 2 demonstrates the real-time mode performance of **npScarf** and **npGraph** via N50 statistics during the assembly of 4 example data sets. This experiment would discover the rate of completing genome assemblies of the new method, set aside the accuracy aspect which had already been discussed previously. **npScarf_wag** basically scaffolds the pre-assembly contigs in the same manner with the original version thus was not discussed here.

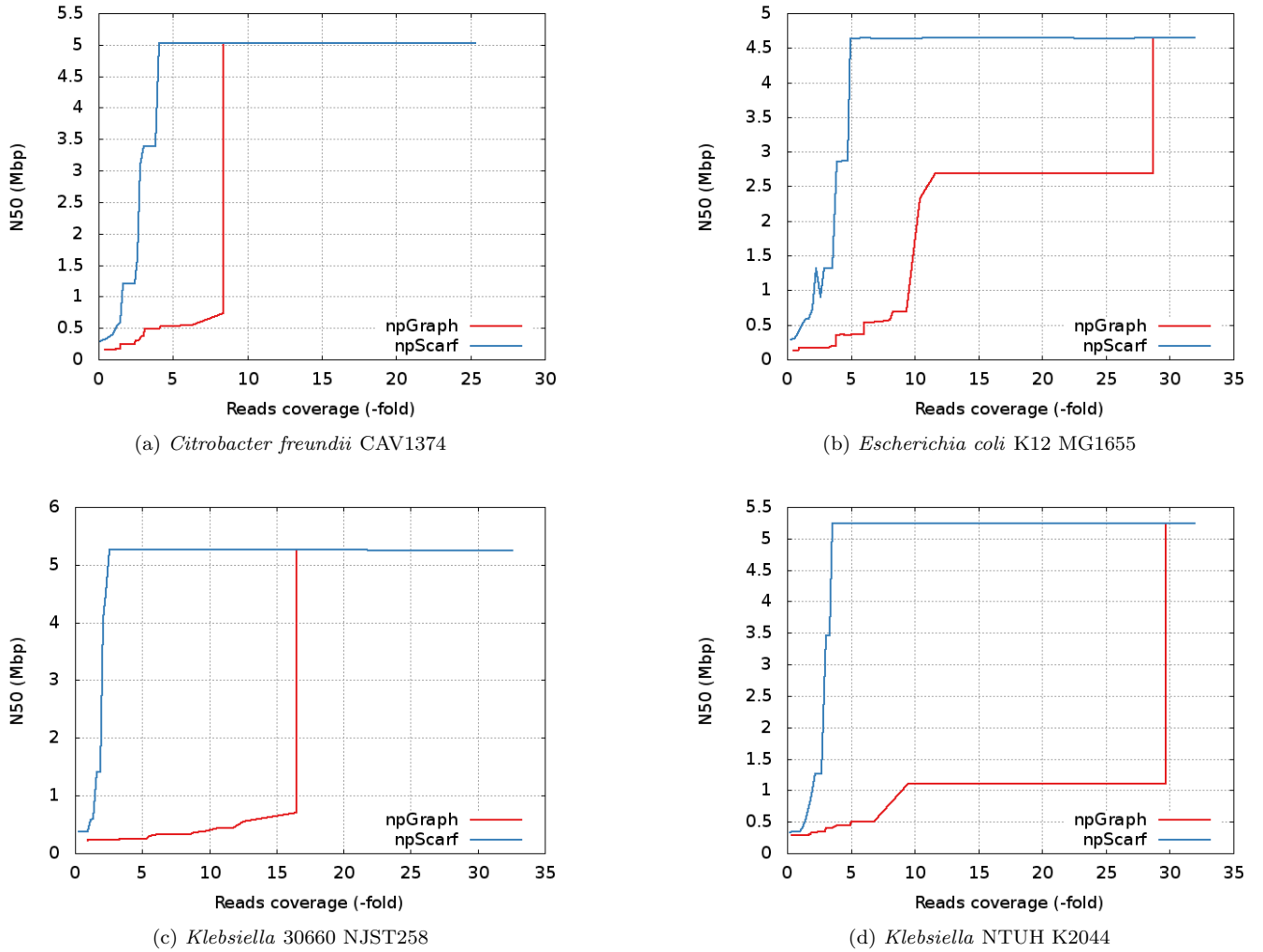


Figure 2: N50 statistics of real-time scaffolding by **npScarf** versus **npGraph**.

As can be observed from all the plots, **npGraph** and **npScarf** both converged to the same ultimate completeness but with different paces and patterns. Apparently it took more data for **npGraph** to finish the same genome than the other. The reason stems from the fact that the new algorithm implemented a more ‘conservative’ approach of bridge construction with at least 3 supporting long-reads for each to prevent any potential mis-bridging. Unlike **npScarf** when the connections could be undone and rectified later if needed, a bridge in **npGraph** will remain unchanged once created. The plot for *E. coli* data clarifies this behaviour when a fluctuation can be observed in **npScarf** assembly at ≈ 3 -folds data coverage. On the other hand, the N50 length of **npGraph** is always a monotonic increasing assembly. The sharp jumping patterns suggested that the linking information from long-read data had been stored and exploited at certain time point decided by the algorithm. Once a unique path has been determined, the bridge can be formed to connect the fragments together into longer sequences.

Metagenomics assembly on mock community

We further employed **npGraph** on mock community data to study the performance of our method in metagenomics co-assembly problem. In this application, sequencing data (including both short and long reads) from mixtures of ten microbial species of ZymoBIOMICS Microbial Community Standards [22] were used as input for **npGraph**. The total genome size was estimated as 61.96 Mbp. There were two settings for the input depending on the distribution of cell abundances in the mixture itself, namely even and log population. On the other hand, 8 out of 10 genomes being sequenced were reconstructed by using PacBio sequencing (RSII and Sequel) previously [23], including *Bacillus subtilis*, *Enterococcus faecalis*, *Escherichia coli*, *Listeria monocytogenes*, *Pseudomonas aeruginosa*, *Saccharomyces cerevisiae*,

Salmonella enterica and *Staphylococcus aureus*. We evaluated the coassembly results by running **metaQUAST** given 8 PacBio assembly as references.

Table 3: Assembly improvement, in terms of NGA50 statistics, from **metaSPAdes** to **npGraph** contigs on two mock communities ZymoLog and ZymoEven [22]. The statistics were generated by **metaQUAST** v3.2 with 8 (out of 10) available PacBio isolate assemblies used as reference [23].

Community	ZymoEven		ZymoLog	
	metaSPAdes	npGraph	metaSPAdes	npGraph
<i>B. subtilis</i>	23,386	382,368	35,390	433,078
<i>E. coli</i>	34,776	1,108,989	—	—
<i>E. faecalis</i>	23,340	217,908	—	—
<i>L. monocytogenes</i>	26,480	520,012	23,146	130,284
<i>P. aeruginosa</i>	59,372	1,753,658	161,816	444,495
<i>S. aureus</i>	26,058	175,908	—	—
<i>S. cerevisiae</i>	—	—	—	—
<i>S. enterica</i>	33,363	4,242,458	—	—

To run **npGraph** on the metagenomics data set, we firstly augmented binning information from using **metaBAT** [24] on the Illumina raw reads, before applying our method to the assembly graph generated by **metaSPAdes**. The default parameter setting was remained as it was for isolate assembly.

In terms of Illumina data, Even community had been sequenced by MiSeq platform which generated about 43-fold coverage while the Log community’s short-read data had been obtained from an Illumina HiSeq 1500, for about 156X coverage. Even though the total amount of base coverage from the latter was almost four-times richer than the former, its **metaSPAdes** assembly quality was lesser. This happened due to the fact of under-presented microbial cells from rare species in the Log population that require much more input for their reads to be sequenced, resulting in significant smaller size of assembly contigs and more fragmented assembly graph (Supplementary Figure 3). The assembly size for the two population are approximately 41 Mbp (66%) and 22 Mbp (36%). During pre-processing step, **npGraph** disregarded nodes which represent short, unconnected and extremely-low-coverage contigs which were indistinguishable from sequencing errors, artifacts or the actual rare species’ genomes without additional works.

Despite of the input graph quality, table 3 shows the assembly improvement in terms of NGA50 after running **npGraph** on the **metaSPAdes** initial graph. As expected from better quality assembly graph, the results for the Even community indicated significant more complete genomes recovered. There were 7 isolate genomes had been identified for this community, compared to only 3 from the more complicated log population. **npGraph** had been able to resolve the assembly graph efficiently for Even community, with the maximum NGA50 improvement for *S. enterica* boosted from 33 Kbp to 4.2 Mbp. On the other hand, genomes from the Log community witnessed increasing length of aligned contigs as well, but not as distinct as for the balanced colony. The longest NGA50 contigs belongs to *P.aeruginosa* of 445 Kbp, however, the counterpart from the Even community was 4-fold than that, at 1.75 Mbp. The only exception was *B. subtilis*, where **npGraph** can only resolved 382 Kbp correct length from the zymo even while the respective statistics was 433 Kbp for the zymo log. However for this isolate, the initial **metaSPAdes** assembly of the former was slightly better compared to the latter’s.

Conclusion

Due to the limits of current sequencing technology, application of hybrid methods should remain a common practice in whole genome assembly for the near future. On the other hand, the ONT platforms are evolving quickly with significant improvement in terms of data accuracy and yield, however, the sequencing cost per base is still high. Beside, the real-time property of this technology has not been sufficiently exploited to match its potential benefits. **npScarf** had been introduced initially to address these issues, however, the accuracy of the assembly output was affected by its greedy alignment-based scaffolding approach. Here we present **npGraph**, a streaming hybrid assembly method working on the DBG assembly graph that is able to finish short-read assembly in real-time while minimizing the errors and mis-assemblies drastically.

Compared to **npScarf**, **npGraph** algorithm employs a less greedy approach based on graph traversal. This might reduce the bridging rate when the linking conditions become more strict, but the concurrent results reported are more reliable. The performance of **npGraph** is comparable to **Unicycler** while consuming much less computational resources so that it can work on streaming mode. Also, the integrated GUI allows users to visualize its animated output in a more efficient way.

In the very first attempt to run real-time assembly on metagenomics data, **npGraph** proved that its method can adapt to scaled-up data and complexity. The assembler was able to handle the De Bruijn assembly graph from Illumina data generated by **metaSPAdes** and simplify it using a minimal input stream of long reads. The result has shown more complete isolate genomes reconstructed out of the graph, but the overall communities’ genome coverage were dropped

with several strains omitted comparing to the reference. The issue is caused by the shortage of short-read sequencing input to cover underrepresented species in the mixture, especially for the Log community.

As a hybrid assembler, similar to **Unicycler**, **npGraph** relies on the initial assembly graph to generate the final assembly. The algorithm operates on the assumption of a high quality assembly from a well-supplied source of short-read data for a decent assembly graph to begin with. It then consumes a just-enough amount of data from a streaming input of nanopore reads to resolve the graph. In summary, extra pre-processing and comprehensive binning for the initial graph could further improve the performance of **npGraph**.

Methods

The work flow of **npGraph** consists of 3 stages: (1) assembly graph preprocessing; (2) graph resolving and simplifying; (3) postprocessing and reporting results. The first step is to load the graph of Illumina contigs and retrieve their metadata which are helpful for the next steps, *e.g.* binning and multiplicity estimation. The second step works on the processed input and augmented information from the previous one. In combination with path inducing from long reads, the assembly graph is then traversed and resolved in real-time. Finally, the graph is subjected to the last attempt of resolving and cleaning, as well as output the final results. The whole process can be managed by using either command-line interface or GUI. Among three phases, only the first one must be performed prior to the MinION sequencing process in a streaming setup. The algorithm works on the assembly graph of Illumina contigs, so the terms *contigs* and *nodes* if not mentioned specifically, would be used interchangeably throughout this context.

Contigs binning

Each population is expected to include contigs of the similar abundance in the final assembly sequences, *e.g.* chromosome, plasmids, or even particular species genome in a metagenomics community. In addition, the binning phase would assist the multiplicity estimation submodule that can differentiate repetitive contigs from unique ones.

Each contig is represented as a single node in the assembly graph and an edge between two nodes indicates their overlap (link) properties. This step is to cluster the biggest nodes (contigs longer than 10Kbp) into different sets, namely *core* groups, based on their degree (number of connections) and coverage values. DBSCAN clustering algorithm [25] is applied for this task by default. The rationale is to approximate a coverage value of a significant contig (which can be splitted into more than 10,000 *k-mers*) to be a sampled mean of a Poisson distribution (of *k-mers* count). The metric is a distance function based on Kullback-Leibner divergence [26], or relative entropy, of two Poisson distributions. Other than that, external binning tools can be employed for more complicated binning task, *e.g.* metagenomics, and the results can be integrated into **npGraph** for better performance. More details can be found on Supplementary Note 1.

Multiplicity estimation

Due to the possible divergence of sequencing coverage relative to the real abundance of sequences, especially for the shorter contigs, an optimization step is carried out to alleviate this issue as shown in Supplementary Note 2. The coverage measures of nodes (which represent contigs) are propagated throughout the graph via connecting edges for calibrations prior to the multiplicity estimation.

Based on the coverage values of all the edges and the graph's topology, we induce the copy numbers of every significant nodes (long contigs) in the final paths. For each node, this could be done by investigating its adjacent edges and answering the questions of how many times it should be visited, from which abundance groups. Multiplicities of insignificant nodes (of sequences with length less than 1,000 bp) can be estimated in the same way but usually with less confidence due to more complicated connections and greater variation of coverage values. For that reason, in **npGraph**'s algorithm, they are only used as augmented information to calculate likelihood scores of candidate paths containing corresponding nodes.

Building bridges in real-time

Bridge is the data structure designed for tracking the possible connections between two anchored nodes (of unique contigs) in the assembly graph. A bridge must start from a unique contig, or *anchor* node, and end at another when completed. Located inbetween are nodes known as *steps* and distances between them are called *spans* of the bridge. Stepping nodes are normally repetitive contigs and indicative for a path finding operation later on. In a complicated assembly graph, the more details the bridge, *a.k.a.* more steps inbetween, the faster and more accurate the linking path it would resolve. A bridge's function is complete when it successfully return the ultimate linking path between 2 anchors.

The real-time bridging method considers the dynamic aspect of multiplicity measures for each node, meaning that a *n*-times repetitive node might become a unique node at certain time point when its (*n* - 1) occurrences have been already identified in other distinct unique paths. Furthermore, the streaming fashion of this method allows the bridge constructions (updating steps and spans) to be carried out progressively so that assembly decisions can be made immediately after having sufficient supporting data. The detail implementation is addressed in Supplementary Note 4.

A bridge in **npGraph** has several completion levels. When created, it must be rooted from an *anchor node* which represents a unique contig (level 1). A bridge is known as fully complete (level 4) if and only if there is a unique path connecting its two anchor nodes from two ends.

Path finding algorithm

Given a bridge with 2 anchors, a path finding algorithm is invoked to find all candidate paths between them. Each of these paths is given a score of alignment-based likelihood which are updated immediately as long as there is an appropriate long read being generated by the sequencer. As more nanopore data arrives, the divergence between candidates' score becomes greater and only the top-scored ones are kept for the next round. We implement a modified stack-based version utilizing Dijkstra's shortest path finding algorithm [27] to reduce the search space when using Depth-First Search (Supplementary Note 5).

It is worth noting that due to dead-ends, there not always exist a path in the assembly graph connecting two anchors as suggested by the alignments. In this case, if enough long reads coverage (20X) are met, a consensus module is invoked and the resulting sequence is contained in a *pseudo* edge.

Graph simplification in real-time

npGraph resolves the graph by reducing its complexity perpetually using the long reads that can be streamed in real-time. Whenever a bridge is finished (with a unique linking path), the assembly graph is *transformed* or *reduced* by replacing its unique path with a composite edge and removing any unique edges (edges coming from unique nodes) along the path. The assembly graph would have at least one edge less than the original after the reduction. The nodes located on the reduced path, other than 2 ends, also have their multiplicities subtracted by one and the bridge is marked as finally resolved without any further modifications.

Result extraction and output

npGraph reports assembly result in real-time by decomposing the assembly graph into a set of longest straight paths (LSP), each of the LSP will present a contig for the result (Supplementary Note 6).

The final assembly output contains files in both FASTA and GFAv1 format (<https://github.com/GFA-spec/GFA-spec>). While the former only retains the actual genome sequences from the final decomposed graph, the latter output file can store almost every properties of the ultimate graph such as nodes, links and potential paths between them.

Other than that, if GUI mode is enabled, basic assembly statistics such as N50, N75, maximal contigs length, number of contigs can be visually reported to the users in real-time beside the Dashboard. The progressive simplification of the assembly graph can also be observed at the same time in the Graph view.

References

- [1] Rozov R, Goldshlager G, Halperin E, Shamir R (2017) Faucet: streaming de novo assembly graph construction. *Bioinformatics* 34(1):147–154.
- [2] Cao MD et al. (2017) Scaffolding and completing genome assemblies in real-time with nanopore sequencing. *Nature Communications* 8:14515.
- [3] Wick RR, Judd LM, Gorrie CL, Holt KE (2017) Unicycler: resolving bacterial genome assemblies from short and long sequencing reads. *PLOS Computational Biology* 13(6):e1005595.
- [4] Giordano F et al. (2017) De novo yeast genome assemblies from MinION, PacBio and MiSeq platforms. *Scientific reports* 7(1):3935.
- [5] Antipov D, Korobeynikov A, McLean JS, Pevzner PA (2016) hybridSPAdes: an algorithm for hybrid assembly of short and long reads. *Bioinformatics* 32(7):1009–1015.
- [6] Prjibelski AD et al. (2014) ExSPAndeR: a universal repeat resolver for DNA fragment assembly. *Bioinformatics* 30(12):i293–i301.
- [7] Bankevich A et al. (2012) SPAdes: A New Genome Assembly Algorithm and Its Applications to Single-Cell Sequencing. *Journal of Computational Biology* 19(5):455–477.
- [8] Zerbino DR, Birney E (2008) Velvet: algorithms for de novo short read assembly using de Bruijn graphs. *Genome research* 18(5):821–9.
- [9] Simpson JT et al. (2009) ABySS: A parallel assembler for short read sequence data. *Genome Research* 19(6):1117–1123.
- [10] Cao MD, Ganesamoorthy D, Cooper MA, Coin LJM (2016) Realtime analysis and visualization of MinION sequencing data with npReader. *Bioinformatics* 32(5):764–766.
- [11] Nguyen SH, Duarte TP, Coin LJ, Cao MD (2017) Real-time demultiplexing Nanopore barcoded sequencing data with npBarcode. *Bioinformatics* 33(24):3988–3990.
- [12] Huang W, Li L, Myers JR, Marth GT (2012) ART: a Next-generation Sequencing Read Simulator. *Bioinformatics* 28(4):593–594.

- [13] Ono Y, Asai K, Hamada M (2012) PBSIM: PacBio Reads Simulator – Toward Accurate Genome Assembly. *Bioinformatics*.
- [14] Mikheenko A, Prjibelski A, Saveliev V, Antipov D, Gurevich A (2018) Versatile genome assembly evaluation with
5 QUAST-LG. *Bioinformatics* 34(13):i142–i150.
- [15] Myers EW et al. (2000) A Whole-Genome Assembly of *Drosophila*. *Science* 287(5461):2196–2204.
- [16] Li H (2013) Aligning sequence reads, clone sequences and assembly contigs with BWA-MEM. p. 3.
- [17] Li H (2016) Minimap and miniasm: fast mapping and de novo assembly for noisy long sequences. *Bioinformatics* 32(14):2103–2110.
- 10 [18] Brudno M et al. (2003) Glocal alignment: finding rearrangements during alignment. *Bioinformatics* 19(suppl_1):i54–i62.
- [19] George S et al. (2017) Resolving plasmid structures in Enterobacteriaceae using the MinION nanopore sequencer: assessment of MinION and MinION/Illumina hybrid data assembly approaches. *Microbial genomics* 3(8).
- [20] Carattoli A et al. (2014) Plasmidfinder and pmlst: in silico detection and typing of plasmids. *Antimicrobial agents
15 and chemotherapy* pp. AAC–02412.
- [21] Potter RF, D’souza AW, Dantas G (2016) The rapid spread of carbapenem-resistant Enterobacteriaceae. *Drug Resistance Updates* 29:30–46.
- [22] Nicholls SM, Quick JC, Tang S, Loman NJ (2019) Ultra-deep, long-read nanopore sequencing of mock microbial community standards. *Gigascience* 8(5):giz043.
- 20 [23] McIntyre AB et al. (2019) Single-molecule sequencing detection of n 6-methyladenine in microbial reference materials. *Nature communications* 10(1):579.
- [24] Kang DD, Froula J, Egan R, Wang Z (2015) MetaBAT, an efficient tool for accurately reconstructing single genomes from complex microbial communities. *PeerJ* 3:e1165.
- [25] Ester M, Kriegel HP, Sander J, Xu X (1996) A density-based algorithm for discovering clusters in large spatial
25 databases with noise. (AAAI Press), pp. 226–231.
- [26] Kullback S, Leibler RA (1951) On information and sufficiency. *The annals of mathematical statistics* 22(1):79–86.
- [27] Dijkstra EW (1959) A note on two problems in connexion with graphs. *Numerische mathematik* 1(1):269–271.